INVITED PAPER *Special Section on Progress towards System Nanotechnology*

Recent Situation of the UV Imprint Lithography and Its Application to the Photonics Devices

Masashi NAKAO[†,††a)], ***Member***

SUMMARY The individual steps of UV imprint lithography have been explained in detail from the points of manufacturing nano-structures. The applications to photonic devices have been also introduced.
key words: *UV-imprint lithography, PDMS, LN filter, dry etching, sapphire substrate, alumina nanohole*

1. Introduction

Optical communication systems with large capacity that support the today's global information and communication society are made up from high-performance photonic devices. To develop higher functional photonic devices, nanotechnology plays an important role for their production. There are two major optical elements of the photonic device, that is, diffraction grating with one-dimensional periodic structure and photonic crystal with two-dimensional periodic structure. In general electron beam lithography (EBL) is used to fabricate the nano-structure on a semiconductor substrate. EBL has also been utilized to produce masks employing in other lithographic technologies, such as photolithography, X-ray lithography, imprint lithography (IL), and others. However, EBL is not suitable for making large-scale microstructure, because the throughput time is extremely low, which corresponds mainly to exposure time of curing EB-resins. The authors have focused on UV imprint lithography (UV-IL), which enables pattern transfer with high-throughput time and comparatively low-cost in order to solve the EBL-problem, and have applied the production process of a diffraction grating for a DFB laser [1]. In this paper, a detailed description of imprinting technique has been made to fabricate fine microstructures on both substrates, lithium niobate and sapphire, which are difficult to produce high-aspect patterns by using conventional method, and some examples for application to photonic devices are mentioned.

Manuscript received August 25, 2015.
Manuscript revised November 13, 2015.
[†]The author is with Micro System Integration Center of Tohoku University, Sendai-shi, 980–0845 Japan.
[††]The author is with Dernaechste Co., Ltd., Atsugi-shi, 243–0036 Japan.
a) E-mail: nakao.masashi@dernaechste.com
DOI: 10.1587/transele.E99.C.333

2. Experimental

2.1 Process of UV Imprint Lithography (UV-IL)

The currently established process of UV-IL is shown in Fig. 1. First, a mold (or a template) is prepared by using techniques of EBL and reactive ion etching (RIE). A resin pattern is formed by EBL on 2-inches or 3-inches of quartz substrates, and the resin pattern is transferred to the quartz substrates by RIE using F-contained gases, such as CF_4, and CHF_3. Figure 2 shows scanning electron microscope (SEM) images of four different quartz molds with various shapes of different period (Λ), height (h), and pillar/pore diameter (ϕ, in case of 2D pattern). These quartz molds are used for fabricating optical devices cited later. Prior to UV-IL, the following pretreatment of the mold is carried out in order to avoid the adhesion of resins on both surfaces of molds and pattern-transferred substrates. Molds are immersed for 10 minutes in SAMLAY-A, which is provided from Nippon Soda Co., Ltd., and they are rinsed for one minute in the solvent of N-Deccan, and are dried by an

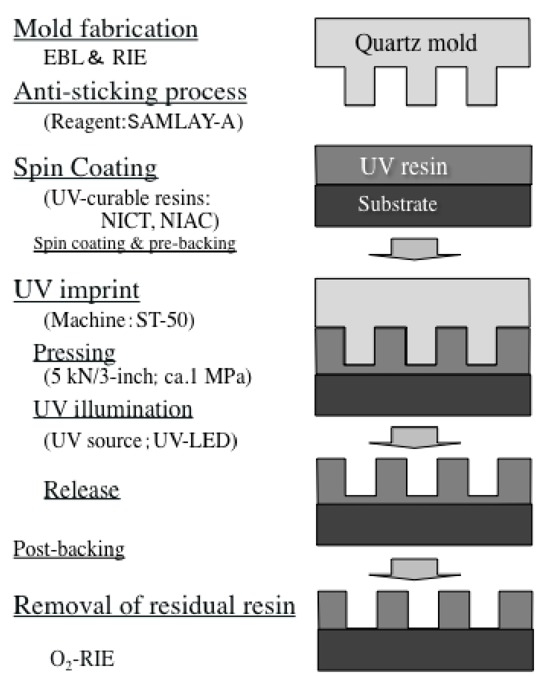

Fig. 1 Pattern transfer process by UV imprint lithography.

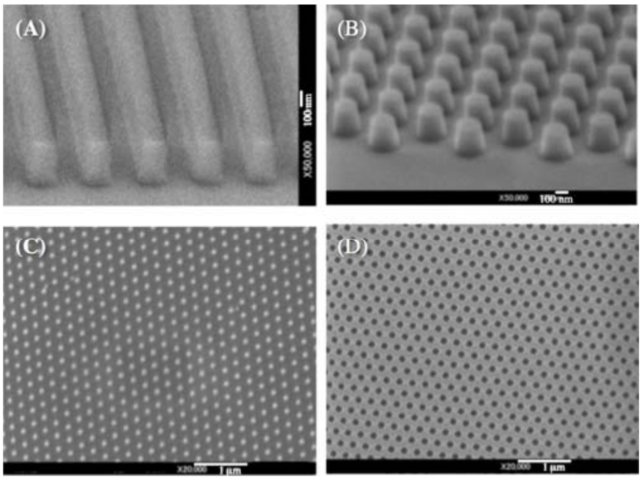

Fig. 2 SEM images of various quartz molds for UV imprint lithography: (A) bird's eye image of 1st-order grating with $\Lambda = 350$ nm and h ~ 250 nm, (B) bird's eye image of 2D pillar array with $\Lambda = 350$ nm, h ~ 340 nm and $\varphi \sim 150$ nm, (C) top view image of 2D pillar array with $\Lambda = 260$ nm, h ~ 270 nm and $\varphi \sim 100$ nm, and (D) top view image of 2D hole array with $\Lambda = 260$ nm, h ~ 200 nm and $\varphi \sim 150$ nm.

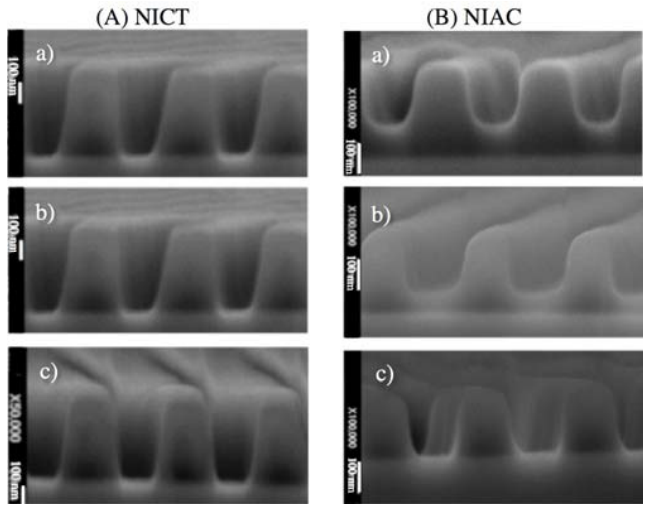

Fig. 3 Cross sectional SEM images of two kinds of resin patterns formed by UV-IL. (A) NICT for the mold ($\Lambda = 500$ nm and h ~ 430 nm): a) b), and c) for 6,000, 4,000, and 2,000 rpm of the rotation rate at spin coating. Pre-backing for 60 sec at 80°C. (B) NIAC for the mold ($\Lambda = 352$ nm and h ~ 220 nm): a) b), and c) for 30, 35, and 40 sec of the pre-backing time at 60°C. Rotation rate at spin coating = 5,000 rpm.

air gun. An anti-sticking layer is formed on the surface of molds. The surface repellency of molds is able to confirm whether water droplets is rolling on the surface of molds into a ball shape. Once the good transfer condition of UV-IL has been found out, reproducible results are obtained by using UV-imprint machine; ST-50, which is manufactured by Toshiba Machine Co., Ltd. The general conditions are as follows; a pressure is almost 1 MPa, and UV-light irradiates for 1 minute with power of 0.3-1 mW/cm^2 from a UV-LED array (wavelength = 365 nm). Two kinds of UV-resin are used for our UV-IL. The resins of NICT and NIAC [2] (both supplied from Daicel Corporation) are named after nano-imprint cationic resin and nano-imprint acrylic resin, and are used for dry etching process and lift-off process, respectively. Usually the imprinted resin of NICT is utilized as a mask for dry etching, then the transfer pattern to the substrate becomes the reversed shape of 凹 and 凸 to the shape of the initial mold. On the other hand, when the solvent-soluble resin, NIAC is used, the transferred pattern on the substrate becomes same unevenness as the shape of the initial mold. Pattern transfer process by NIAC will be later mentioned as lift-off process. It is important to control the thickness of the resin according to the pattern height of the quartz mold in order to minimize the thickness of the residual resin layer (RRL) after UV-IL. The thinner thickness of RRL is the better to preserve the resin shape. The initial thickness of NICT is controlled by the rotation rate of the spin coating as shown in Fig. 3 (A), and in the case of NIAC the pre-backing time is changed into controlling the thickness as shown in Fig. 3 (B). Because of the high volatility of the NIAC monomer, the thickness of the RRL changes from 80 nm in the pre-baking time is 30 seconds to almost zero at 40 seconds. In the case of NIAC resin, the baking time is easier and more reproducible way to control the film thickness than the rotation speed of spin coating. The RRL is removed by O_2-RIE. The resin shape can be maintained by using Inductive Coupled Plasma (ICP)-type RIE as compared with Capacitive Coupled Plasma (CCP)-type RIE as shown in Fig. 4, because ICP-RIE is anisotropic etching method. In general, imprint process is performed as the thickness of RRL will be less than 50 nm, and O_2-RIE for about 10 seconds is generally carried out to create isolated resin pattern on the substrate. For convenience CCP-RIE is usually used due to the short process time and it is convenient. ICP-RIE is used when the shape retention is important.

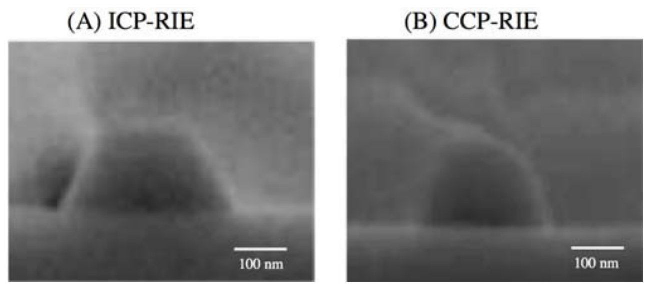

Fig. 4 Changes in the resin shape due to two different residual films processing by ICP-RIE and CCP-RIE by using O_2 for 10 sec.

2.2 Lift-Off Process

It is possible to form metal pattern on a substrate by combination of UV-IL and lift-off process. The pattern transfer process on the substrate via metal-mask formation is overviewed in Fig. 5. Electron beam deposition of a metal is carried out on the substrate with the resin pattern formed by UV-IL (see Fig. 1). The thickness of the deposited metal film is preferably set to less than one third of the height of the UV resin. After metal deposition, the resin is taken off

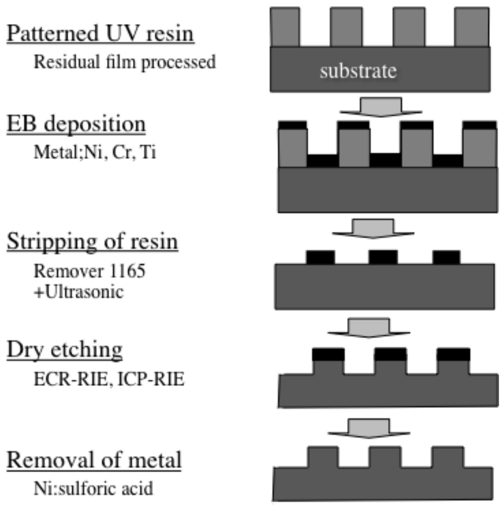

Fig. 5 Pattern transfer process to a substrate using a lift-off method.

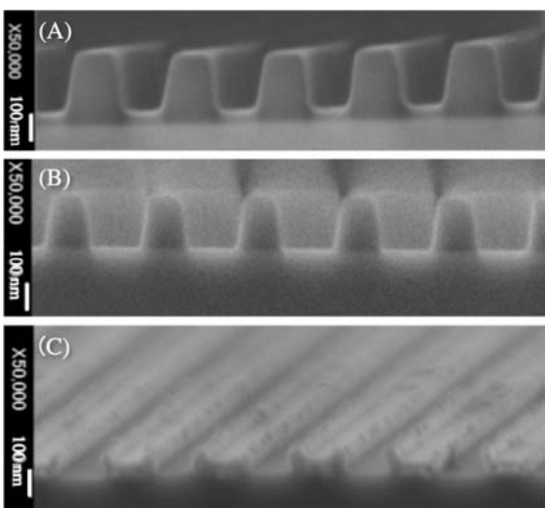

Fig. 6 Formation of the metal pattern by UV-IL and a lift-off method. Cross sectional SEM images; (A) After UV-IL. (B) After O_2-RIE. (C) After lift-off process.

by ultrasonic cleaning in a remover 1165.

The author mainly uses Ni as the metal, because Ni is suitable for the dry etching with high selectivity and it can be easily removed by sulfuric acid after dry etching. Figure 6 shows SEM images of the Ni pattern formation process using UV-IL lift-off method. The mold used here is the grating pattern in Fig. 2 (A). By UV IL, a resin pattern with height of 220 nm is formed. And there remains 40 nm of RRL. The RRL is completely removed by processing of O_2-RIE, and the grating height becomes 185 nm. Then, EB deposition is carried out to prospect a thickness of about one-third of pattern height, and finally Ni pattern with a thickness of 60 nm is obtained. Although both sides of the Ni stripe are in the spike-like forms (Fig. 6 (C)), which have little influence on the transferred stripe pattern of the substrate by dry etching. Metal patterning has been improved by devising deposition process as shown in Fig. 7, where patterning of three kinds of metal, Cr, Ni and Ti have been demonstrated with almost

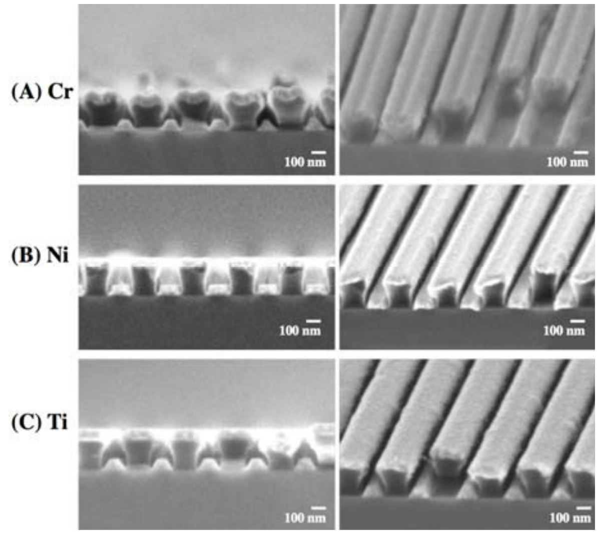

Fig. 7 Formation of three kinds of metal patterns by UV-IL and lift-off method. Cross-sectional (left) and bird's-eye view (right) SEM images.

same thickness of 80 nm. These trapezoid type metal patterns can be achieved by controlling deposition rate and deposition interval. Using this technique, it is also applicable to the formation of the metal wire with thin film and good adhesion nature on the substrate. Aluminum patterning is also already realized in the same way. In the case of aluminum the thin film formation by sputtering is carried out in place of EB evaporation.

2.3 PDMS Mold Formation

Although quartz mold have good durability, it cannot be avoided against contamination and/or degradation of fine pattern during repeated use. When the quartz mold becomes contaminated due to resin-adhesion after many times of UV imprint process, cleaning of the molds is done by an excimer light irradiation to be effective already been reported [3]. The excimer light (wavelength = 172 nm) efficiently generates a singlet oxygen from a oxygen molecule. The singlet oxygen can remove the resin accumulating in the mold of the groove. Mold corruption occurs especially in the case of narrow nano-pattern with high aspect. Therefore, it is general to prepare a replica from the master mold. Polydimethylsiloxane (PDMS) is generally used as replica molds for UV-imprint [4]. Recently Shin-Etsu Chemical Co., Ltd. provides UV-curable PDMS (UV-PDMS), which becomes the trigger of solidification. One can easily fabricate PDMS mold by using the same process as UV imprint technology when the UV-PDMS is used instead of the UV resins of Fig. 1. Furthermore, PDMS mold has the following advantages. That is, it is possible to prepare a PDMS mold from an impermeable substrate such as Si, and the PDMS mold is used as a mold of UV imprint. By using the duplicated PDMS mold (a daughter mold) instead of quartz mold, UV imprint technique becomes more effective transfer method of nano-pattern. Figure 8 shows example of pattern trans-

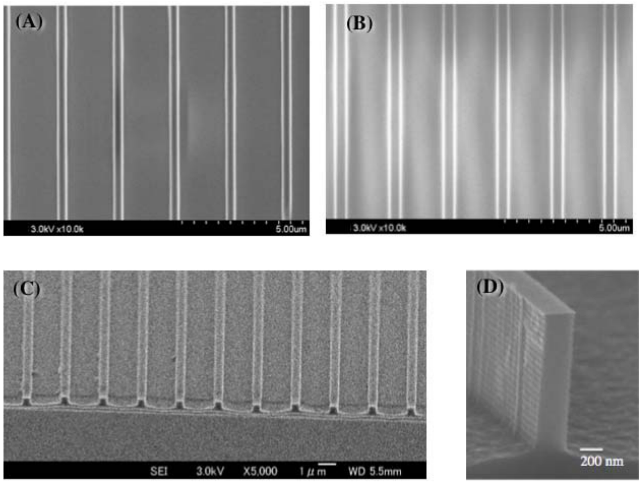

Fig. 8 Example of pattern transfer process to Si substrate via PDMS mold. Top view SEM images of the Quartz mold (A, 凸-pattern) and the PDMS mold (B, 凹-pattern), and bird's eye SEM images of the NICT resin (C) and the etched Si substrate (D).

fer process to the Si substrate via PDMS mold; SEM image of A is quartz mold with 凸-type stripe pattern, B is the PDMS mold, C is the NICT resin, D is the Si pattern fabricated by the deep-RIE and is 凸-type as same as the quartz mold. Whole pattern transferring proceeds successfully. The PDMS mold has following some advantages: It does not adhere to the UV resin, then anti-sticking treatment is unnecessary. It minimizes the effect of dust between mold and transferred substrate due to its flexibility. One can perform imprint process in the air without influence of air bubble because of its air permeability. It is easily cleaned with an organic solvent.

2.4 Alumina Nanoholes and Their Transformation

The authors have realized alumina nano-holes having a high aspect two-dimensional periodic structure [5], by using anodic oxidation of aluminum with periodic concave pattern on the surface formed by imprinting. At the time of imprinting, the SiC substrate with two-dimensional convex pattern such as Fig. 2 (C) is used to avoid mold damage. A short period of alumina nanohole may be useful as an initial mold for the application, and that can be achieved by use of period reduction technique [6]. The author has succeeded in fabricating 30 nm- and 50 nm-period alumina nano-hole arrays as shown in Fig. 9. The former is to 3 mm square area latter is realized in 5 mm square size. A diameter of these pores are less than 10 nm. By using UV-imprint technique, pattern transfer to PDMS of the alumina nano-hole is carried out, and further transfer to UV resin is done from the PDMS mold. Successful duplication of nanostructure is observed in Fig. 10, which shows the surface SEM image (A) of PDMS transferred from alumina mold of Fig. 9 (B) and the resin surface SEM image (B) formed from the PDMS mold. From the transferred PDMS pattern, the depth of the alumina nanohole is estimated to be about 20 nm. The depth

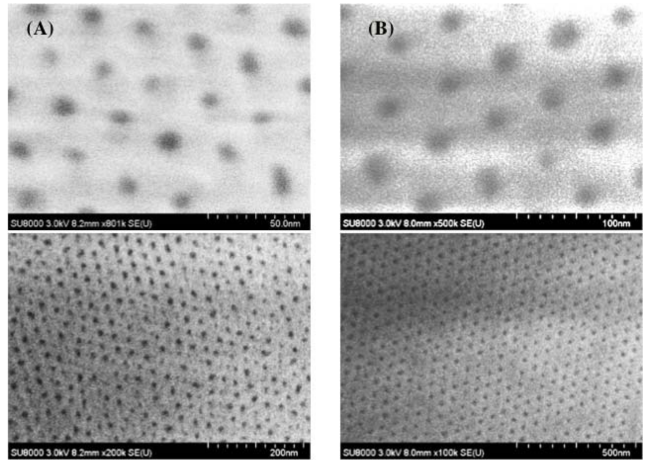

Fig. 9 Top view SEM images of alumina nanohole with pitch of 30 nm (A) and 50 nm (B). Magnification changes in the up and down.

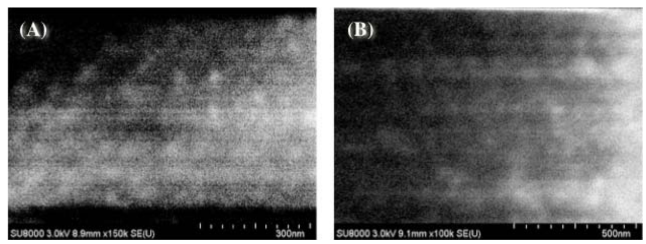

Fig. 10 Top view SEM images of PDMS (A) and UV-resin (B) with 50 nm pitch.

is basically controlled by the electrolysis time. It results in the transfer of nanometer size.

3. Results and Device Applications

By utilizing the fabrication techniques described above, the authors have performed various device applications. Two application examples are introduced for which production has been difficult by conventional lithography.

3.1 Grating Formation on the Lithium Niobate (LN) Substrate and Application to LN Filter Wave Guide

LN has been used in practical as a modulator for changing the electrical signals into optical signals in optical communication. However, since the electron beam is strongly influenced by the ferroelectric behavior of the material, it is not easy to form the nanostructures LN surface by EBL [7]. The authors have prepared a diffraction grating for wavelength filter waveguide formed on the LN substrate by Ti diffusion by using UV-imprint technique combined with lift-off method, and have successfully fabricated ridge-type waveguide with an insertion loss of 23 dB [8]. This value is high enough to do the filtering of wavelength. Quartz mold is used herein as shown in Fig. 2 (A). Etching of the LN has been performed by an electron cyclotron resonance (ECR)-RIE using CF_4 and the Ni pattern as a mask. The etching

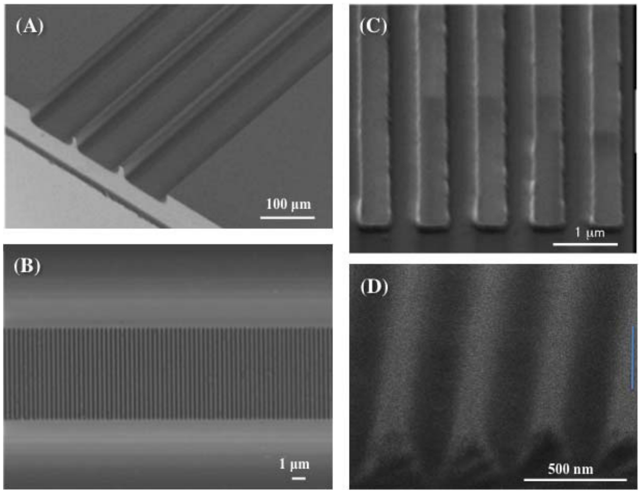

Fig. 11 SEM images of grating formed on the LN waveguide: (A) Bird's eye view, (B) Top view, (C) Top view covered with Ni, and (D) Cross-sectional image.

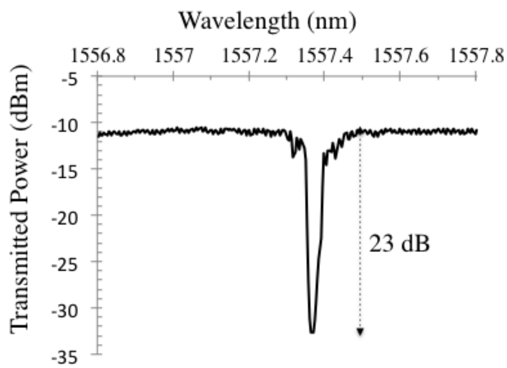

Fig. 12 Filter characteristics of the LN waveguide.

rate of LN is 9.7 nm/min, and that of Ni is 1.4 nm/min, that is about 7 in selectivity, which is capable to form a relatively deep diffraction grating on the LN substrate. A diffraction grating having a period of 352 nm is shown in Fig. 11. Figure 12 is the filter characteristic with a fine insertion loss of 23 dB, and Fig. 13 is the filter array characteristics. In the case of LN, the optical waveguides formed by the dicing method. In Fig. 11 (A) two optical waveguides are formed in order to clarify the filter characteristics by comparing the presence or absence of the diffraction grating. To make the 20 integrated filter array, the period of the diffraction grating in the optical waveguide was increased from 350.2 nm to 354 nm by 0.2 nm increments. The distance of each waveguide is 250 μm. Change of filtering wavelengths in Fig. 13 reflects the changing value the period of diffraction, which is able to realize the filter wavelength change by about 1 nm. Figure 13 also indicates that the filtering wavelength depends on the change of the width of the optical waveguide (w_{WG}), and that is due to the change of the effective refractive index. By using here-developed technology it is expected to realize the wavelength selective modulator with additional function to simple on/off. It would be also applied to ferroelectric elements such as polarization reversal elements and surface acoustic wave (SAW) elements.

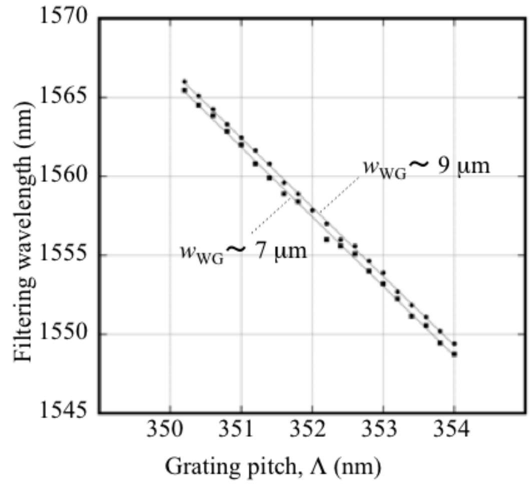

Fig. 13 Filtering characteristics of the LN filter arrays.

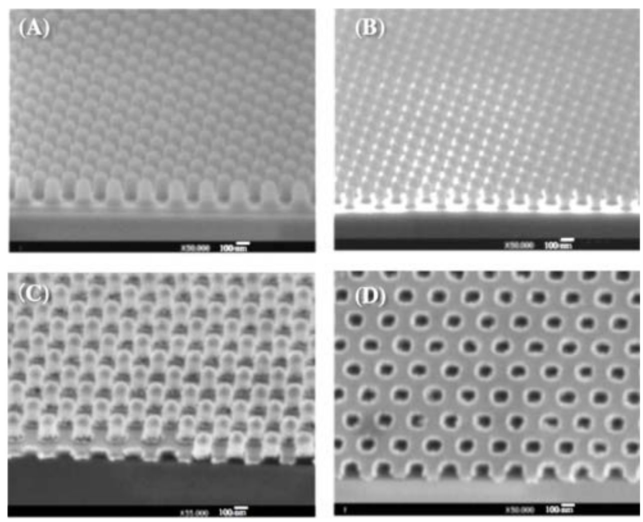

Fig. 14 Bird's eye view SEM images of manufacturing process of Ni hole array: (A) UV resin after UV-IL, (B) After O_2-RIE, (C) After Ni deposition, and (D) Ni hole array.

3.2 Formations of Metal Hole Array and the Photonic Crystal Structure to the Sapphire Substrate

Low cost is required for mass production of a photonic crystal structure on the sapphire substrate, which serves as a base substrate in order to increase the extraction efficiency of the light of GaN-based LED. Etching of the sapphire substrate is not easy. When the resin is used as a mask, it is necessary to make high aspect structure and is difficult in relative. The authors have approached to make the photonic crystal structure on the sapphire substrate by using new developing method as mentioned below. Figure 14 shows the manufacturing process developed by metal hole array. Quartz mold used here has triangular type of two-

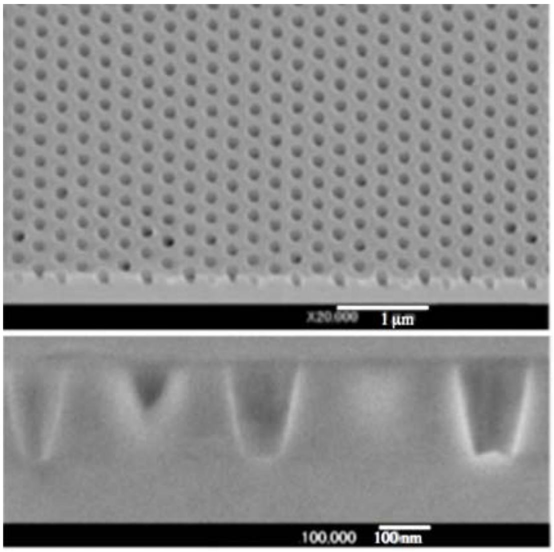

Fig. 15 SEM images of a nanohole array formed on a sapphire substrate; Bird's-eye view image (above) and cross-sectional image (blow).

dimensional hole array structure as shown Fig. 2 (D) with period = 260 nm, depth∼200 nm, hole diameter∼150 nm. First, the pillar structure, such as Fig. 14 (A) is formed by UV-IL. The pillar array of resin becomes completely independent on a substrate by the residual film treatment of O_2-RIE as shown Fig. 14 (B). About 60 nm depositing Ni is done by the EB evaporation method, and the entire substrate surface is covered with Ni as shown Fig. 14 (C). And Ni hole array with the same structure as the quartz mold is formed when the UV resin is remove by remover 1165 (Fig. 14 (D)). Etching selectivity of sapphire to Ni is more than 3. The etching of the sapphire substrate covered by the Ni-hole array mask is done by ICP-RIE for 11 minutes. BCl_3 and Cl_2, are used as etching gases. The etching depth is 190 nm as shown in Fig. 15. 2D-hole array is realized in the area of 40 mm on the 2 inches sapphire substrate. Finally the layer structure of GaN-based LED [9] is fabricated on the opposite side of the sapphire substrate with photonic crystal structure. The light output of the LED increases by a few percent as compared without photonic crystal structure. Effect of various 2D-pattern is still under investigating.

4. Conclusions

Recently, UV-imprint technology is applying to plasmonic devices using nano-periodic structure of the metal and the insulator [10]. Nanostructure fabrication technologies introduced here are seemed to be the best way to achieve new optical devices [11]. In the future, fusing of photonics and electronics on a nanometer scale is expected, and the imprint technology here introduced would be useful and suitable technology to realize new devices.

Acknowledgments

The author is grateful to the National Institute of Information and Communications Technology (NICT) and Micro System Integration Center of Tohoku University for supporting this work.

References

[1] S. Ishizuka, M. Nakao, S. Mashiko, J. Mizuno, and S. Shoji, "Fabrication of Uniform Gratings on Composite Semiconductors Using UV Nanoimprint Lithography," J. Photopolymer Sci. Tech., vol.22, no.2, pp.213–217, 2009.

[2] T. Nishino, N. Fujii, H. Miyake, T. Yukawa, J. Sakamoto, R. Suzuki, H. Kawata, and Y. Hirai, "Metal Liftoff Process using Solvent Soluble Resist by UV-NIL," J. Photopolym. Sci. Tech., vol.23, no.1, pp.87–90, 2010.

[3] M. Nakao, M. Yamaguchi, and S. Yabu, "IMPRINT-MOLD-CLEANING BY VACUUM ULTRAVIOLET LIGHT," J. Nonlinear Optic. Phys. Mat., vol.19, no.4, pp.773–779, 2010.

[4] H. Shinohara, H. Goto, T. Kasahara, and J. Mizuno, "Fabrication of a Polymer High-Aspect-Ratio Pillar Array Using UV Imprinting," Micromachines, vol.4, no.2, pp.157–167, 2013.

[5] H. Masuda, H. Yamada, M. Satoh, H. Asoh, M. Nakao, and T. Amamura, "Highly ordered nanochannel-array architecture in anodic alumina," Appl. Phys. Lett., vol.71, no.19, p.2770, 1997.

[6] S. Shingubara, S. Maruo, T. Yamashita, M. Nakao, and T. Shimizu, "Reduction of pitch of nanohole array by self-organizing anodic oxidation after nanoimprinting," Micro-electron. Engineer., vol.87, no.5-8, pp.1451–1454, 2010.

[7] S. Shinada, T. Kawanishi, T. Sakamoto, and M. Izutsu, "An optical grating filter dry-etched on a LiNbO3 substrate," IEICE Express Letter, vol.3, no.14, pp.347–352, 2006.

[8] M. Nakao, S. Nakajima, S. Shinada, and T. Kawanishi, Proc. 25th Int. Micro. Nanotech. Conf., 1P-7-74, 2012.

[9] H. Hirayama, N. Noguchi, and N. Kamata, "222 nm Deep-Ultraviolet AlGaN Quantum Well Light-Emitting Diode with Vertical Emission Properties," Appl. Phys. Express, vol.3, no.3, p.032102, 2010.

[10] B. Choi, M. Iwanaga, H.T. Miyazaki, K. Sakoda, and Y. Sugimoto, "Photoluminescence-enhanced plasmonic substrates fabricated by nanoimprint lithography," J. Micro/Nanolith. MEMS MOEMS, vol.13, no.2, p.023007_1, 2014.

[11] H.T. Miyazaki, T. Kasaya, H. Oosato, Y. Sugimoto, B. Choi, M. Iwanaga, and K. Sakoda, "HASH(0x50d029c)," Sci. Tech. Adv. Mater., vol.16, no.3, p.035005, 2015.

Masashi Nakao received master's and doctor's degrees in synthetic chemistry from the University of Tokyo in 1979 and 1984, respectively. In 1985, he joined the Opto-electrical Device Section of NTT Research laboratories, Atsugi, Japan. At NTT he had been engaged in research and development of semiconductor lasers for fiber communication for 21 years. From 2007 to 2012, he was a senior researcher of the National Institute of Information and Communications Technology, NICT, and he was investigating new functional photonic devices by using imprint lithography. He has retired in 2012, and now is a part-time lecturer at Tohoku University, Nihon University, and Waseda University.